# Formulation and Physico-mechanical Characterization of an Eco-mortar Composite Based on Bottom Ash and Magnetized Water

Redouane Mghaiouini[1,2,*], Abderrazzak Graich[2], Anis Elaoud[3], Toufik Garmim[2], M.E. Belghiti[5], Nisrine Benzbiria[6], Mahmoud Hozayn[4], Mohamade Monkade[2] and Abdeslam El Bouari[1]

[1]Department of Chemistry, Physical Chemistry Laboratory Applied Materials, Faculty of Sciences-Ben M'sik, Hassan II University, Casablanca, Morocco
[2]Department of Physics, Condensed Matter Laboratory, Faculty of Sciences, Chouaib Doukkali University, El-jadida, Morocco
[3]Laboratory of Environmental Sciences and Technologies, University of Carthages, Higher Institute of Sciences and Technology of Environment, Tunisia
[4]Agronomy Dept., Agric. and Biol. Div., National Research Centre, El-Bohoth St., 12622 Dokki, Cairo, Egypt
[5]Laboratory of Nernest Technology, 163 Willington Street, Sherbrook, J1H5C Quebec, Canada
[6]Laboratory of Interface Materials and Environment, Faculty of Sciences Aïn Chock, Hassan II University, Casablanca, Morocco

**\*Author for correspondence:**
Redouane Mghaiouini ✉ filagri1.maroc@gmail.com 📍 Department of Chemistry, Physical Chemistry Laboratory Applied Materials, Faculty of Sciences-Ben M'sik, Hassan II University, Casablanca, Morocco

## Abstract

**Objectives**: To study the influence of electromagnetic fields on the physico-mechanical properties of the mortar (resistance to compression and bending). **Methods/analysis**: In the current research, the influence of the electromagnetic field in the mortar was studied experimentally by replacing the cement with 10% bottom ash provided from a thermal power plant and formulates a mortar with high resistance to compression and bending. Scanning electron microscopy (SEM)/X-ray diffraction (XRD) analyses were further performed to confirm the obtained results. **Findings**: Based on the above results, it was found that the use of magnetized water offered better microstructure and mechanical resistance to compression and bending, for both normal mortar and mortar containing 10% of bottom ash from thermal power plants. The majority of previous publications were produced on normal mortars based on cement and ordinary water, while this study was carried out on mortars with magnetized water and bottom ash. **Novelty /improvement**: A new method was proposed for the formulation of an eco-mortar based on bottom ash obtained from thermal power plant and magnetized water. Water mortar magnetizes with bottom ash to provide several

Redouane Mghaiouini, Abderrazzak Graich, Anis Elaoud, Toufik Garmim, M.E. Belghiti,
Nisrine Benzbiria, Mahmoud Hozayn, Mohamade Monkade and Abdeslam El Bouari

uses in the field of civil engineering which includes better recovery of industrial waste, an efficient material, and a reduction in the use of cement in the mortar.

# 1. Introduction

The hydration of the cement is done in a faster and active way because the magnetic field decreases the size of the clusters of water molecules which gives water this capacity to penetrate easily inside the particles of cement [1], which improves the resistance of concrete. The storage of magnetized water in a basin can probably last up to 12 hours. However, over this space of time, the magnetization can be weakened or canceled [2–3]. The study by Ref. [4] showed that when mortar is kneaded with magnetic water, the characteristics of the mortar and cement paste are enhanced. The magnetic field improves the compressive strength of concrete and also the distribution of pore size [1]. In Refs. [5–8], authors analyzed the workability and the compressive strength of the mortar and concrete prepared with granulated blast furnace slag and magnetized water. Results showed that the compressive strength of mortars formulated with magnetic water was improved by 9% to 19% more than those prepared with tap water. The compressive strength of concrete formulated with magnetic water was improved by 10–23% more than that of mortars with tap water. It was also found that the magnetic water improved the flow of the mortar and the hydration of the concrete. [7, 9–11]. The literature review showed that the potential use of cement is mainly determined by its physical characteristics such as particle size, coloring potential, etc. Indeed, the coarse and glassy structure of the bottom ash makes it a perfect substitute for natural materials [12]. It is still used as an economical substitute for more expensive sand in concrete manufacturing. Furthermore, bottom ash is also introduced as a basic constituent in road construction [13]. Earlier researches showed that bottom ash was also used in ceramic [14] and bricks manufacturing [15–16]. It was shown that coal cement used as a partial substitute for cement with a 10% substitution rate increased the compressive strength compared to ordinary cement at all ages. In the present study, a drop in resistance was observed with a rate higher than 10%; however, the resistance became again superior to ordinary cement only up to 56 days of cure. In Ref. [17], Monse also showed that ground clinker can effectively substitute up to 20% of a cement, without reducing the strength class of that cement.

# 2. Materials and Methods

## 2.1. Mortar Preparation

Mortar is a composite material, essentially made up of a mixture of three ingredients: sand, hydraulic binder (cement or lime), and water, which is generally tap water. In this study, the bottom ash (BA) is introduced into the formulation of the cement mortar by replacing it

with different percentages of BA with BA/cement mass ratios equal to: 10%. To determine the mechanical properties, the mortars were prepared according to the European standard NF EN 196-1 which requires the normal mortar to be composed in mass, of a portion of cement (450 g), three portions of sand (1350 g) and half a portion of water (225 g), i.e. with a water/cement ratio W/C equal to 0.5. The ingredients were mixed in accordance with the requirements of the standard for 4 min in a 5 L mixer at temperature ambient and at a relative humidity higher than 50% [18]. Before starting the mechanical study; the mortars were prepared in the form of prismatic test pieces with the dimensions 4*4*16 cm$^3$ as shown in Figure 1. The samples thus formed were stored in open air. Then, these test pieces were tested after 28 days by mechanical resistance to bending and compression.

Table 1 shows the complete formulation of the mortars. M0 mortar is the normal mortar that we take as a reference. The M10 mortar was obtained by replacing part of the cement with bottom ash quantities of 10% by mass.



**FIGURE 1.** Mortar specimens.

**TABLE 1.** Mortar formulation with bottom ash

| Elements | % Bottom ash | Cement (g) | Sand (g) | Water (g) |
|----------|--------------|------------|----------|-----------|
| 1.92 | 52.07 | 405 | 1350 | 225 |

## 2.2. Analysis of the Materials to be Used

### 2.2.1. Cement

The cement used in the formulation of mortars is CEM II (CPJ 45) defined in the Moroccan standard NM 10.1.004. It is a Portland cement made up of 81.5% clinker, 12% limestone; the rest is gypsum which regulates the setting.

The chemical composition of CPJ 45 cement is presented in Table 2 below:

**TABLE 2.** Mortar formulation with bottom ash

| Cement | % $SiO_2$ | % $Al_2O_3$ | % $Fe_2O_3$ | % CaO | % MgO | % $SO_3$ | % $K_2O$ | LOI |
|--------|-----------|-------------|-------------|-------|-------|----------|----------|-----|
| CPJ 45 | 17 | 5 | 3 | 63 | 2.3 | 3.33 | 1.2 | 5.17 |

## 2.2.2. Sand

The sand used in the mixtures was taken from the coast (Oualidia). Its particle size analysis was carried out according to standard NF P18-560 with an electric sieve shaker. The results obtained are summarized in Figure 2.
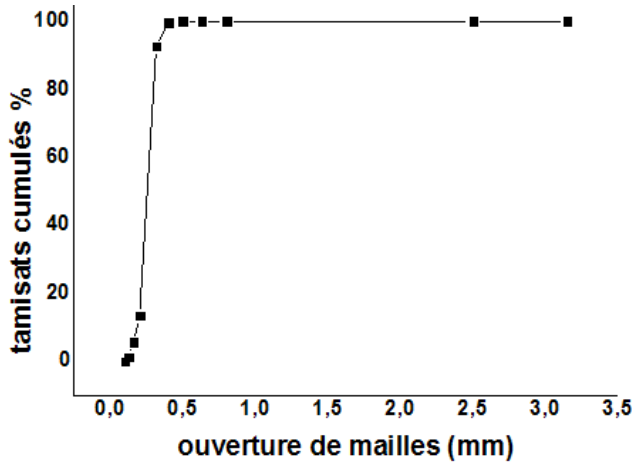


**FIGURE 2.**　Particle size curve of the sand.

According to the grain size curve, the corresponding uniformity coefficient Cu is 1.7 and the predominant grain size ranges from 0.2 mm to 0.315 mm. The sand used is therefore uniform and composed mainly of fine grains. The apparent density of the sand used was determined, considering a proportion of pores (voids) of 41.5%. The results obtained are summarized in table3:

The actual density obtained of 2.77 g/cm$^3$ corresponds well to the specific weight of sand.

**TABLE 3.**　Chemical composition of CPJ45 cement

| Bulk density without compaction | Bulk density with compaction | Real density |
|---|---|---|
| 1.43 g/cm$^3$ | 1.54 g/cm$^3$ | 2.77 g/cm$^3$ |

## 2.2.3. Coal Bottom Ash

The results of analysis of the chemical composition of the JLEC bottom ash are given in Table 4.

It is noted that more than 80% of the chemical constitutions of the ashes were composed of the constants $SiO_2$, $Al_2O_3$, and $Fe_2O_3$, with regard to lime the mineralogical

**TABLE 4.**　Densities of the used sand

| CaO | SiO$_2$ | Fe$_2$O$_3$ | Al$_2$O$_3$ | K$_2$O | Na$_2$O | ZnO | PbO | SO$_3$ | MgO | CaO$_{free}$ | LOI |
|---|---|---|---|---|---|---|---|---|---|---|---|
| 1.92 | 52.07 | 8.86 | 23.34 | 1.9 | 0.4 | 0.01 | 0.01 | 1.87 | 1.09 | 0.29 | 8.24 |

composition of the bottom ash contains 2% maximum of this element as indicated by the X-ray diffraction technique. This study reveals the existence of two peaks. The first is attributed to the quartz ($SiO_2$) and the second corresponds to the mullite (Figure 3).
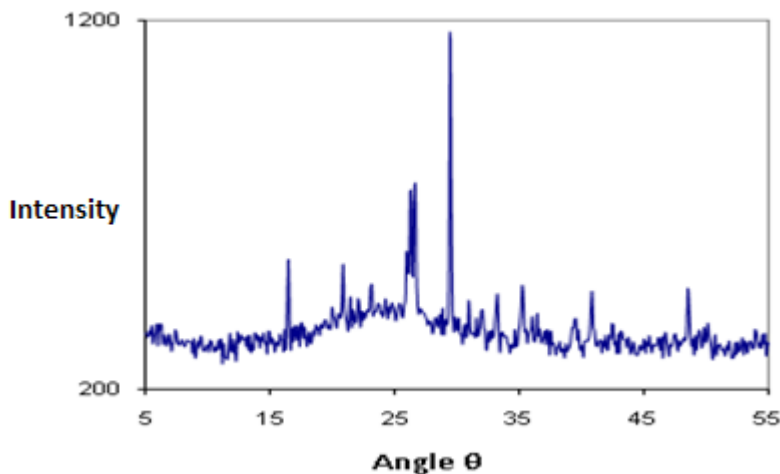


**FIGURE 3.** Mineralogical spectrum of bottom ash.

This result can be explained by the mineralogy of the coal used, which generally consists of crystalline silica in the form of quartz and phyllitheous minerals from the group of clays (schists) [19].

The study of the morphology of bottom ash was carried out using Philips XL 30 ESEM scanning electron microscope (SEM).

Figure 4 illustrates the morphological structure of the crude bottom ash obtained before filtration: they are in the form of spherical particles of irregular sizes. This result is similar to the one reported by Wei-ling Sun et al. [20] , who showed by SEM micrographs that the observed irregularity reveals the presence of porosity. The authors also showed
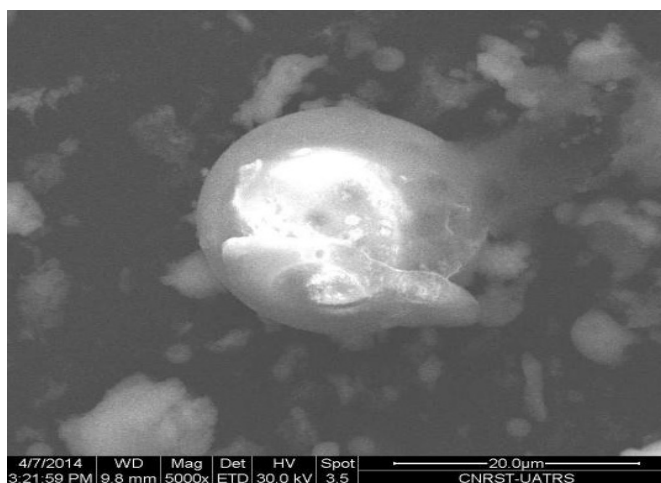


**FIGURE 4.** Bottom ash morphology.

that most of the cement grains were in the form of hollow spheres or spheres filled with smaller spheres. Micro crystals are also observed at the surface of the particles, which may indicate the presence of mullite and quartz. The elements Si, Al, Ca, Na, and small amounts of Fe are contained in the pledospheres. This is consistent with our mineralogical spectrum depicted in Figure 3 which chemical composition is illustrated in Table 2. It can also be pointed out that the specific surface area measured for these crude bottom ash (400 $m^2$/kg) remains low compared with that of fly ash.

## 2.3. Mechanical Study: Method

### 2.3.1. Study of Mechanical Resistance to Bending

The experimental determination of the mechanical flexural strength of mortars was carried out on a material characterization machine provided with a three-point bending device as shown in Figure 5 [21]. The experimental conditions used are described by standard EN 196-1.
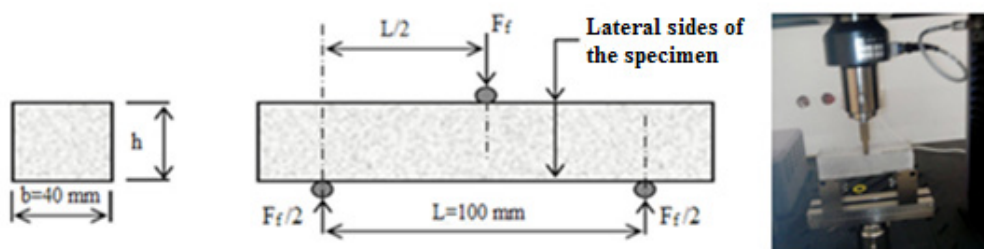


**FIGURE 5.**   Mechanical bending strength test device.

The test piece is placed symmetrically on the terminals of the support so that the path of the force is perpendicular to the longitudinal axis of the test piece. A preload was applied to avoid any specimen play and to balance the displacement measurement device. In order to obtain the breaking load, the increasing force $F$ is applied to the upper face of our specimen at a constant speed of 1 mm/min until the prism breaks. We then deduce the mechanical resistance to bending given by:

$$R_f = \frac{3F_f L}{2bh^2}$$

### 2.3.2. Mechanical Resistance to Compression

After flexural, we re-use each half-prism to measure the mechanical resistance to compression (Figure 6) [21].

A progressive force was applied on the transverse section (4 × 4 $cm^2$) of the test piece with the same speed until the breaking load from which the mechanical resistance to compression was calculated in mega-Pascal using the following formula:
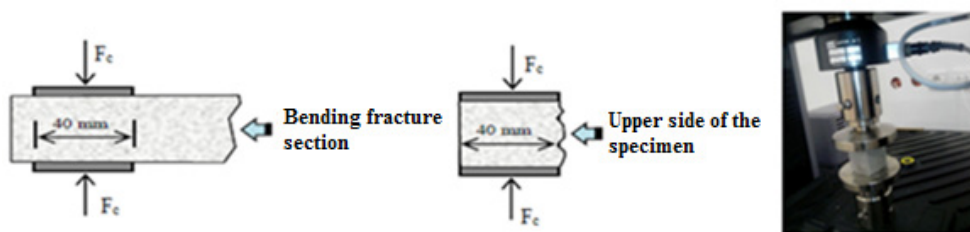
**FIGURE 6.** Mechanical compressive strength test device.

$$R_c = \frac{F_c}{b * h}$$

Afterwards, the specimens were also analyzed a diffract meter of flat technical form at the university of Chouaib Doukkali El Jadida Morocco, using a copper anticathode (Cu-Kα) with wavelength λ equal to 1. 5406 A. The specimens after crushing were analyzed by a IRTF type Thermo.

## 2.3.3. Experimental Variables

Tap water is treated through a kind electromagnetic field by the System Aqua 4D. Figure 7 shows the electromagnetic field generator machine developed for this research. The length of this machine is 804 mm and its weight is about 2 kg. The diameter of the drain hose is 112 mm. The water flow can be adjusted using a proportional integral differential regulator (PID). The system is a set composed of the following modules:

- The F Pro command that brains the system. It generates processing signals and continuously checks the proper functioning of the system.
- The processing units (TU) which diffuse the signals generated by the F Pro control into the water.

When tap water passes through this electromagnetic field, it turns into EMFTW as shown in Figure 7.

The water to cement ratio (W/CM) of the mortar samples is 0.5. For mortar specimen, the percentage of cement substituted by bottom ash is equal to 10%.

# 3. Results and Discussion

## 3.1. Mechanical Characterization of Mortars

Figures 8 and 9 respectively illustrate the mechanical behavior of flexural and compressive strengths of mortars prepared with tap water (TW) and magnetized water (MW) after 28 days of hardening.

Figures 10 and 11 experimentally explain another mechanical parameters of the mortar which are flexural and compressive resistances after 28 days of hardening of specimens
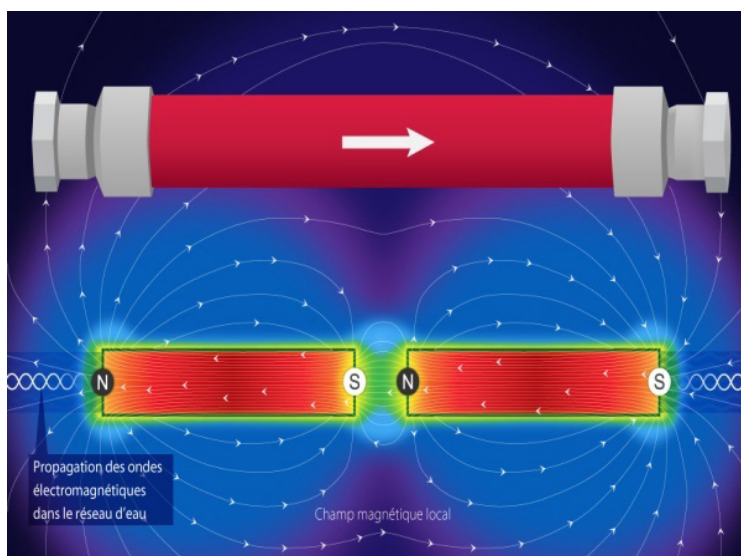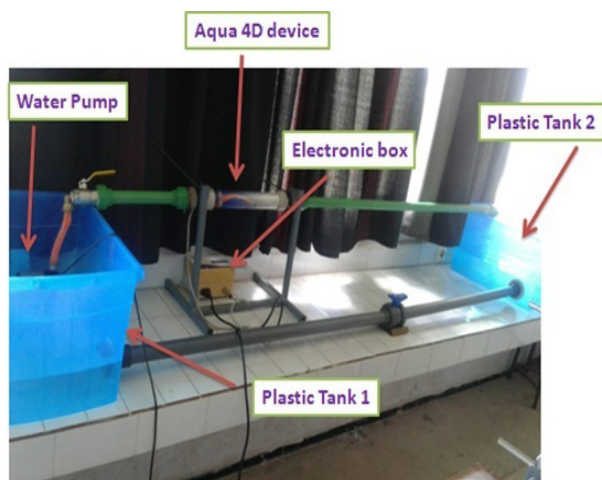
**FIGURE 7.**   Image of the device generating an electromagnetic field.

containing 10% of BA mixed with tap water (TW) and magnetized water (MW). Although prepared with varying percentages of bottom ash substitution of cement, all of the mortar specimens show a similar evolution, indicating that the effect of EMFTW magnetic field strength on resistance to the compression of different mortar specimens is almost identical. As it can be seen, if bottom ash is used instead of cement and regardless of the bottom ash content, flexural and compression strength of the mortar mixed with EMFTW is greater than those of the control (the tap water being represented by 0 T). In other words, EMFTW is more effective than tap water during the hydration process. In addition, the effect of EMFTW on compressive strength varies with the percentage of bottom ash. The greatest growth is noticed when working with 10% bottom ash.
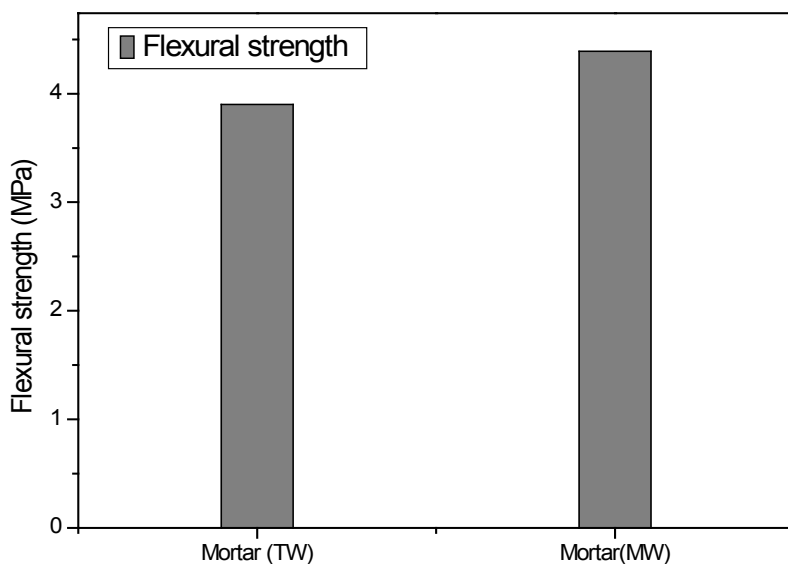
**FIGURE 8.** Flexural strength of mortar prepared with (TW) and with magnetized tap
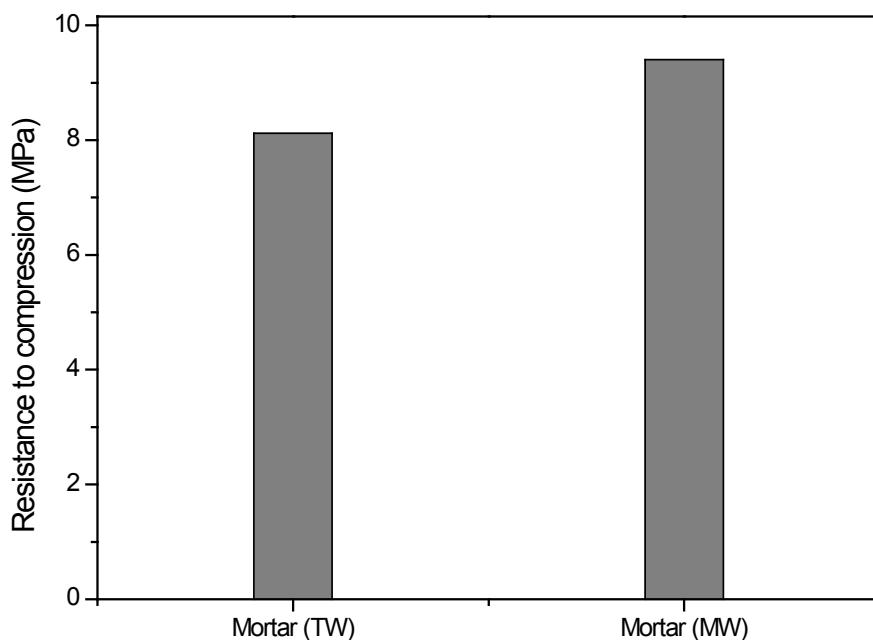water (MW).



**FIGURE 9.** Compressive strength of mortar prepared with (TW) and with magnetized tap
water (MW).

Inside the electromagnetic field generated by AQUA 4 D, the magnetic force can
fragment small clusters of water into clusters. As a result, the efficiency of water increases
[20]. As does the hydration of the cement grains, the speed of distribution and penetration
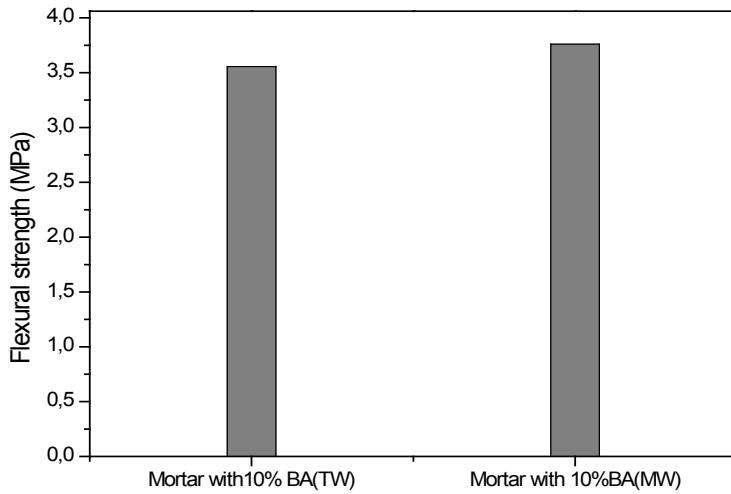
**FIGURE 10.** Flexural strength of the mortar prepared with BA 10% (TW) and with BA 10% (MW).
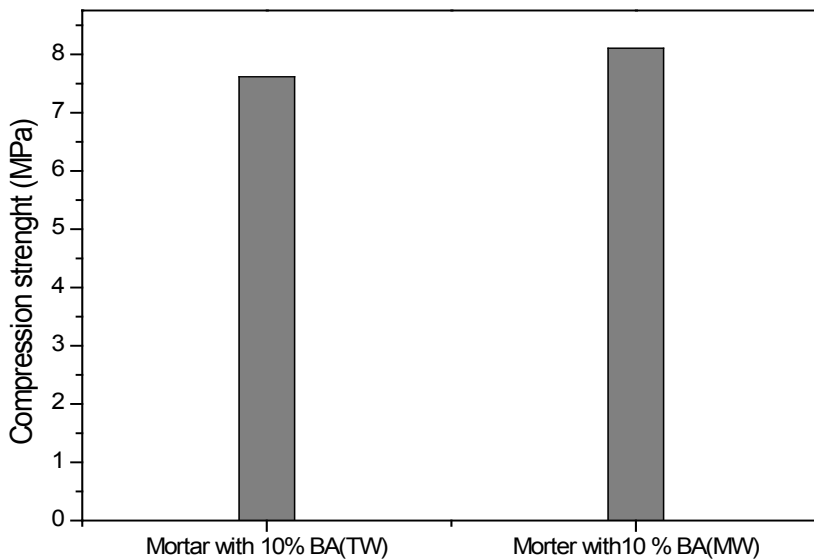


**FIGURE 11.** Compression strength of the mortar prepared with BA 10% (TW) and with BA 10% (MW).

of EMFTW through the almost impermeable layer of the cement paste is greater than that of tap water. As a result, the hydration is improved, which increases the strength of the mortar. Furthermore, during the hydration the clusters of magnetized water become smaller. This induces their dispersion and facilitates their penetration through the particles of cement which improves the reaction of water with the cement and increases the interface water magnetized with particles of sand and bottom ash [7, 22–23]. It is also interesting

to mention that the mortar manufactured by EMFTW contains fewer micro pores as it is denser and therefore less permeability of water through the mortar is expected [24].

## 3.2. Characterization of Mortars by X-ray Spectroscopy

From the X-ray diffraction pattern presented in Figure 12, three main phases are identified which consist of calcium carbonate phase ($CaCO_3$) observed at positions (2 theta) (23.01°; 29.37°; 35.98°; 39.41°; 43.14°; 47.28°; 48.49°), silicon oxide ($SiO_2$) revealed at positions (2 theta) (20.79°; 26.60°; 39.41°; 40.17°; 45.83°; 50.04°; 59.93°; 68.07°) and finally iron oxide phase ($Fe_2O_3$) at position (2 theta) (18.03°).

The X-ray diffraction diagram illustrated in Figure 13 shows that the crystalline phase consists mainly of calcium carbonate phase ($CaCO_3$) noted at positions (2 theta) (23.04°; 29.41°; 36.02°; 39.44°; 47.45°; 57.42°), silicon oxide ($SiO_2$) revealed at positions (2 theta) (20.85°; 26.63°; 50.15°). Two new phases are identified in the mortars prepared with (MW) which are attributed to the $Mg_3(SO_4)_2(OH)_2$ phase at positions (2 theta) (27.5°, 34.1°) and the $Al_2CaO_8SiO_4$ phase at the positions (2 theta) (28. 04°).

## 3.3. Interpretation of IR results

From Figures 14 and 15, a band around 525.53 cm$^{-1}$ (Si–O–Si) is observed which corresponds respectively to the valence vibration and deformation modes of the Si–O (silica phase) layer C3S and C2S. Moreover, an intense peak around 976, 73 cm$^{-1}$ shows a very precise percentage of cement. A bung towards 875 cm$^{-1}$ is also revealed, followed by a changeable peak towards 872, 83 cm$^{-1}$ followed in turn by a peak which changes around 1409, 87 cm$^{-1}$, characteristic of the modes of vibration of elongation of the C–O. These



**FIGURE 12.** X-Ray diffraction diagram of diffraction of mortars prepared with TW and MW.

**FIGURE 13.** X-Ray diffraction diagram of mortar (10 % BA) mixed with TW and MW.

absorption peaks are characteristic of the existence of calcium carbonate ($CaCO_3$) perhaps formed by a carbonation reaction of cement. On the contrary, the bands characteristic of the aluminates phase are invisible on the infrared spectrum. An analysis of the infrared



**FIGURE 14.** Infrared spectroscopy spectrum of mortars prepared with TW and MW.
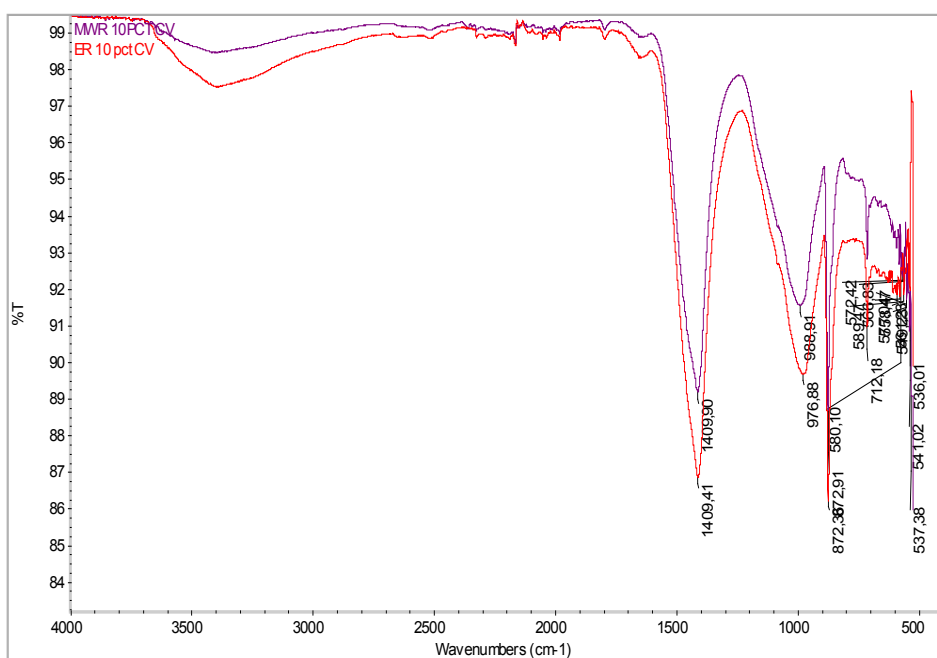
**FIGURE 15.** Infrared spectroscopy spectrum of mortar (10% BA) mixed with TW and MW.

spectra of Figures 14 and 15 shows the elongation of the SO layer of sulfates ($SO_4^{2-}$) to 614 $cm^{-1}$ revealing the existence of gypsum ($CaSO_4$).

Furthermore, the peaks revealing water ($H_2O$) appear above 3000 $cm^{-1}$ (around 3386 $cm^{-1}$) alongside a peak relative to an elongation vibration mode of the OH layer. In Figure 15, hearth ash (pozzolan) present in small quantity in the composite to analyze is not detected. This component is generally determined by a wide and intense vibration of the Si–O silica layer at 1030 $cm^{-1}$. In fact, hearth ash is completely camouflaged by the clinker, which makes it very difficult to detect this phase by IR technique [25].

**TABLE 5.** Physicochemical analysis of tap water and magnetized water

| Settings | Tap water | Magnetized water |
|---|---|---|
| pH | 7.69 | 8.25 |
| Conductivity | 1695 µS/Cm | 971 µS/Cm |
| TDS | 848 mg/l | 485 mg/l |
| Salinity | 0.85 PSU | 0.48 PSU |
| Ca | 78.5 mg/l | 79 mg/l |
| Oxydability | 0.41 mg/l | 0.49 g/l |
| Chlorure | 88.5 mg/l | 89 mg/l |
| Temperature | 17.8 °C | 17.1 °C |
| Mg | 23.83 mg/l | 23.9 mg/l |
| Alkalinity | 10.35 °F | 10.4 °F |
| TH or hydrometric titer | 2.94 meq/l | 2.98 meq/l |
| Ammonium | 0 mg/l | 0 mg/l |
| Iron | 0 mg/l | 0 mg/l |

# 4. Conclusion

This research was to develop the bottom ash which is a waste of thermal centrals in the field of materials construction. This research focused on replacing a part of cement with this waste harmful to the environment. In the course of this study, several conclusions were made:

In an experimental way, it was shown that the use of magnetized water improved the mechanical properties of normal bottom ash mortars compared to that with 0% of magnetized water. Mortar mixed with magnetized water was improved by 12.56% compared to the one mixed with tap water. In the case of the asserted mortar with 10% bottom ash and magnetized water, flexural strength was improved by 12.67% compared to mortar mixed with 10% bottom ash and tap water.

The compressive strength of normal mortar formulated with magnetized water was enhanced by 5.91% compared to mortar mixed with tap water.

For the asserted mortar with 10% bottom ash and magnetized water, compressive strength increased by 6.42% if compared to mortar mixed with 10% bottom ash and tap water.

Adding bottom ash in the formulation of an eco-mortar seems to be a solution that takes into account both environmental, economic and growing global demand for building materials.

# References

1. Su N, Wu YH, Mar CY. Effect of magnetic water on the engineering properties of concrete containing granulated blast-furnace. *Cement Slag and Concrete Research*. 2000, 30(4), 599–605. https://doi.org/10.1016/S0008-8846(00)00215-5

2. Fu W, Wang Z. The new technology of concrete engineering. The Publishing House of Chinese Architectural Industry: Beijing. 1994. http://www.techn-opress.org/fulltext/j_acc/acc5_2/acc0502001.pdf

3. Mghaiouini R, Elaoud A, Garmim T, Belghiti ME, Valette E, Faure CH, Hozayn M, Monkade M, El Bouari A. The electromagnetic memory of water at kinetic condition. *International Journal of Current Engineering and Technology*. 2020, 11–18. https://doi.org/10.14741/ijcet/v.10.1.3

4. Wang L, Zhao S. Laboratory studies on the properties of cement-based. 2008. https://www.researchgate.net/publication/291840045_Laboratory_studies_on_the_properties_of_cement-based_materials_with_magnetic_water

5. Wei H, Wang Y, Luo J. Influence of magnetic water on early-age shrinkage cracking of concrete. *Construction and Building Materials*. 2017, 147, 91–100. DOI: 10.1016/j.conbuildmat.2017.04.140.

6. Ghorbani S, Tao Z, De Brito J, Tavakkolizadeh M. Effect of magnetized water on foam stability and compressive strength of foam concrete. *Construction and Building Materials*. 2019, 197, 280–290. DOI: 10.1016/j.conbuildmat.2018.11.160.

7. Ghorbani S, Gholizadeh M, de Brito J. Effect of magnetized water on the mechanical and durability properties of concrete block pavers. *Materials*. 2018, 11(9), 1647. DOI: 10.3390/ma11091647.

8. Siva Konda Reddy B, Vaishali G, Ghorpadeand H, Rao S. Influence of magnetic water on strength properties of concrete. *Indian Journal of Science and Technology*. 2014, 7(1), 14–18. http://www.indjst.org/index.php/indjst/article/view/46674

9. Esfahani AR, Reis MI, Mohr B. Magnetized water effect on compressive strength and dosage of super plasticizers and water in self-compacting concrete. *Journal of Materials in Civil Engineering*. 2018, 30(3), 04018008. DOI: 10.1061/(ASCE)MT.1943-5533.0002174.

10. Ahmed HI. Behavior of magnetic concrete incorporated with Egyptian nano alumina. *Construction and Building Materials*. 2017, 150, 404–408. https://doi.org/10.1016/j.conbuildmat.2017.06.022

11. Gholhaki M, Hajforoush M, Kazemi M, An investigation on the fresh and hardened properties of self-compacting concrete incorporating magnetic water with various pozzolanic. *Materials, Construction and Building Materials*. 2018, 158, 173–180. https://doi.org/10.1016/j.conbuildmat.2017.09.135

12. Yu Q, Sugita S, Sawayama K, Soijma Y. Effect of electronic water hardening and electronic hardening on concrete resistance. *Cement and Concrete Research*. 1998, 28, 1201–1208.

13. Cheriaf M, Cavalcante JR, Pera J. Pozzolanic properties of pulverized coal combustion bottom ash. *Cement and Concrete Research*. 1999, 29, 1387–1391. https://doi.org/10.1016/s0008-8846(99)00098-8

14. Lemeshev VG, Gubin IK, Savel'ev YA, Tumanov DV, Lemeshev DO. Utilization of coal-mining waste in the production of building ceramic materials. Translated from Steklo iKeramika. 2004. https://link.springer.com/article/10.1023/B:GLAC.0000048698.58664.97

15. Asokan P, Mohini S, Asolekar SR. Coal combustion residues – environmental implications and recycling potentials. *Resources, Conservation and Recycling*. 2005, 43, 239–262. https://doi.org/10.1016/j.resconrec.2004.06.003

16. Haldun K, Mine K. Usage of coal combustion bottom ash in concrete mixture. *Construction and Building Materials*. 2007, 1922–1928. https://doi.org/10.1016/j.conbuildmat.2007.07.008

17. Monse B. Thermo-chemo-hydro-mechanical behavior of petroleum cement at a very young age under HP/HT conditions: experimental approach and analysis by change of scale. *Engineering Sciences*. University of Paris-Est. 2010. https://patents.google.com/patent/FR2987128A1/en

18. Zalaghi B, Lamchouri F, Toufik H, Merzoukia M. Valorization of natural porous materialsin the treatment of leachate from the landfill uncontrolled city of Taza. *Journal of Materials and Environmental Science*. 2014, 5(5), 1643–1652. https://www.jmaterenvironsci.com/Document/vol5/vol5_N5/201-JMES-953-2014-Zalaghi.pdf

19. Fan M, Brown R, Wheelock TD, Cooper AT, Nomura M, Zhuang Y. Production of a complex coagulant from fly ash. *Chemical Engineering Journal*. 2005, 6, 269–277. https://doi.org/10.1016/j.cej.2004.12.044

20. Su N, Wu CF. Effect of magnetic field treated water on mortar and concrete containing fly ash. *Cement & Concrete Composites*. 1999, 29, 1387–1391. https://doi.org/10.1016/S0958-9465(02)00098-7

21. Aarfane A, Salhi A, El Krati M, Tahiri S, Monkade M, Lhadi EK, Bensitel M. Kinetic and thermodynamic study of the adsorption of Red195 and methylene blue dyes on fly ash andbottom ash in aqueous medium. *Journal of Materials and Environmental Science*. 2014, 5(6), 1927–1939. https://www.researchgate.net/publication/273764865_Etude_cinetique_et_thermodynamique_de_l&#39;adsorption_des_colorants_Red195_et_Bleu_de_methylene_en_milieu_aqueux_sur_les_cendres_volantes_et_les_machefers_Kinetic_and_thermodynamic_study_of_the_adsorption

22. Juan J, Bernal S, Mota RG, Candelas IR, Jose A. Lozano O. Effects of static magnetic fields on the physical, mechanical, and microstructural properties of cement paste. *Hindawi Publishing Corporation Advances in Materials Science and Engineering*. 2015, 9. http://dx.doi. org/10.1155/2015/934195

23. Abdel-Magid TIM, Hamdan RM, Abdelgader AAB, Omer MEA, Ahmed NMR. Effect of magnetized water on workability and compressive strength of concrete. *Procedia Engineering*. 2017, 193, 494–500. DOI: 10.1016/j.proeng.2017.06.242.

24. An-Tai Ma. Effect of magnetic water on engineering properties of self –compacting concrete with waste catalyst. A thesis submitted to institute of construction National Yunlin University of Science and Technology in partial fulfillment of the requirement for degree of Master of Design in Construction Engineering Taiwan-Republic of China. 2007. DOI: 10.13140/ RG.2.2.35245.38880.

25. Fargas F, TouZePh. The IRTF spectrometer, an interesting method for the characterization of cements. *Bulletin from the Bridges and Carriageways Laboratories*. 2001, 77–88.